IEEE Access
Multidisciplinary | Rapid Review | Open Access Journal

Received October 11, 2018, accepted October 21, 2018, date of publication October 30, 2018, date of current version November 30, 2018.

Digital Object Identifier 10.1109/ACCESS.2018.2878554

Design and Application of Fractional Order Predictive Functional Control for Industrial Heating Furnace

XIAOMIN HU[1], QIN ZOU[2], AND HONGBO ZOU[2]
[1]School of Science, Hangzhou Dianzi University, Hangzhou 310018, China
[2]Information and Control Institute, Hangzhou Dianzi University, Hangzhou 310018, China

Corresponding author: Hongbo Zou (zouhb@hdu.edu.cn)

ABSTRACT This paper proposes a fractional order predictive functional control method for temperature control of an industrial electric heating furnace. Since the electric heating furnace is affected by complex factors such as measurement noise, uncertainty, model/plant mismatches, and so on, it is more important to derive accurate modeling and controller design for improved control performance. Under the uncertain facts, conventional control methods based on integer order models may not offer the desirable control performance. The fractional order model of the heating furnace based on the input-output data of the step response test is introduced to describe the dynamics of the process and the Oustaloup approximation is used to transform the fractional order process into an integer formulation. Then a predictive functional controller is designed through minimizing the future predicted output error based on the state space model transformation. Application has been implemented on the industrial heating furnace and the experimental tests reveal the validity of the proposed controller in comparison with conventional integer model-based PFC.

INDEX TERMS Industrial electric heating furnace, fractional order systems, predictive functional control, step-response modeling.

I. INTRODUCTION

In industrial processes, there is a common usage of the industrial heating furnaces in the industrial productions, such as drying, polymerizing, metal melting, and other physical-chemical processes [1]. Since the temperature process of the electric heating furnaces is characterized with large inertia, time delay, and uncertainty, it is difficult for traditional control methods to meet the increasing requirements on control performance improvement that directly influence the product quality [2]. The classical control, such as proportional-integral-derivative (PID), is widely used for its simplicity and convenience [3]. The internal model PID control is one of the well-known effective methods and is still a hot control topic for industrial process applications and research in recent years [4], [5]. However, for the large inertia and time-delay processes, it may take a long time for the PID control system to achieve the steady state and cannot meet the increasing requirements on control performance properly.

Model predictive control (MPC), which is one of the advanced control strategies for industrial processes, is a practical one in the industrial process control filed since it was proposed in the last century [6]–[8]. For example, MPC based on the extended state space model was successful applied for the temperature control [9] and batch processes [10]. MPC for the benzene hydrogenation via reactive distillation to overcome the performance of sluggish responses and reject disturbance was illustrated in [11]. Also, in [12], MPC strategy in which the measurements of the input disturbances and the output observer have been taken into consideration for the solar boreal thermal system was presented. These achievements in industrial processes illuminate the improved performance using MPC methods. Among these methods, predictive functional control (PFC) is one of the major branches of MPC and was proposed by Richalet, et al. for industrial dynamic systems and successful applications in industry also illustrate the practicality of this algorithm [13]–[15]. Subsequently, several studies on PFC have been proposed prosperously due to its favorable performance and the simplified calculation by solving the difference between the desired trajectory and the predicted output. The representative research issues are briefly summarized as follows. In [16], an efficient application on the parallel

mechanisms using PFC scheme was implemented with the enlightened disturbance rejection and tracking performance. In [17], the two dimensional PFC for batch processes was implemented. Self-adaptive PFC for exothermic batch reactor [18] and the other practical applications [19], [20] were properly and efficiently employed for industrial process control systems. Also, in the recent two years, robust PFC algorithms based on dead-time variations has been presented to deal with non-integrative stable processes [21]. Based on Hammerstein identified model and genetic algorithm, PFC strategy was developed and applied for the turntable servo system in [22]. In [23], pole-placement PFC was proposed to improve the tuning for systems with significant underdamped modes.

Nevertheless, most of these model-based predictive control strategies are on the general integer order models of the processes. As indicated in [24], the fractional order models, which may better govern the properties of lossy transmission, heat conduction process, neutron flux dynamics in a nuclear reaction and etc., are much more effective to characterize the processes because of involving the extra fractional order operator compared with integer order models. As the general predictive control based on mathematical integer-order models may fail to guarantee favorable performance for complex heating processes, the motivation of research on fractional order systems and control design is to exploit new methods to obtain better performance in practical applications. In the field of industrial automation, the fractional order modeling and fractional order control are the hot research directions of the fractional order calculus [25]–[27]. Studies on fractional order calculus focus on the accurate description of the processes and the expected improvement of the controllers by using additional fractional-order parameters. The aforementioned issues regarding fractional order modeling or fractional order control can be the successful factual arguments to support this view. Also, some efficient implementations of fractional order controllers in industrial applications were presented in [28]. The optimization performance of the fractional order robust PID controllers based on generalized isodamping approach as well as gain-scheduling algorithm also been displayed in the experiments in [29]. In [30], according to the fractional order modeling and control for the dynamic processes, the authors came to a conclusion about the inevitable huge space of the fractional order calculus to explore new and interesting contents.

Not only for classical control, research on fractional order calculus has also enjoyed the glow of the development of MPC strategies. In [31], the PFC based on the extended nonminimal state space model was successfully used for fractional order system and the excellent performance revealed the effectiveness of the fractional order predictive control. In [32], the state space PFC, where two basic functions were introduced into the control variable, was presented for fractional order control systems. In [33] and [34], the new fractional-order generalized predictive controllers (GPC) with the fractional order integral operators involved in the cost functions has been proved to enhance the performance of the control systems. In [35], the practical application on fractional-order thermal systems using MPC algorithm illustrated the efficiency of the method. Combined with the merits of both the fractional order PID algorithm and predictive control algorithms, the controllers based on the time domain were designed to improve the performance [36], [37]. Also in [38], to guarantee the satisfaction of state and input constraints, the authors presented a tube-based MPC algorithm for the fractional order systems. Even though most of these achievements address the theoretical research well, however, there are still needs for efforts to be focused on actual industrial applications [39]–[41].

As it is known for us that the model-based predictive control algorithms depend on the precise and suitable models to characterize the process. From the previous research, the fractional order calculus can provide a new possibility to adequately describe the characteristics of the practical processes, and the fractional order model has become a growing demand for accurate models to describe the real processes. In this paper, the study is to propose a new fractional order PFC for the practical temperature process and validate the improvement of this proposed scheme by experimental tests. For the practical application, the implementation of the temperature control using fractional order PFC algorithm has been performed on the electric heating furnace. In view of the complexity of modeling by dynamic mechanism, the step-response input-output data have been sampled to derive the fractional order model and integer order model of the temperature process. For the fractional process, the Oustaloup approximation is introduced to obtain the discrete model, and then the state space model, which is further derived from the discrete model. Finally, the chosen state variable is used to evaluate the difference between the future predicted outputs and the expected outputs. By minimizing the difference, the manipulated variable is obtained for the practical process. Compared with traditional PID and PFC based on integer order models, the experimental results show the improvement and effectiveness of the proposed FPFC.

II. PROCESS DESCRIPTION

The dynamic characteristics of the temperature process are always affected by a great diversity of factors, for instance, pressure variations of the furnace as well as physical properties change of the heating wire. For the overall consideration of these factors, the precise model can be more complicated and difficult for the design of the controller. Thus, the simple step-response models based on the measured output and input data are derived.

In this section, modeling for the electric heating furnace will be formulated briefly as follows. The first order plus dead time model [8] is considered for the conventional predictive functional controller

$$G_1(s) = \frac{K_1 e^{-\tau_1 s}}{T_1 s + 1} \tag{1}$$

where, K_1, T_1, τ_1 are the process gain, time constant and time delay, respectively.

The corresponding fractional order model is chosen as the following form

$$G_2(s) = \frac{K_2 e^{-\tau_2 s}}{T_2 s^{\alpha} + 1} \tag{2}$$

where, α is the order of the fractional model $G_2(s)$, K_2, T_2, τ_2 are the corresponding parameters.

In this study, the steady state gain, K_1, is derived through the change of the steady value of the output and the change of the input value. T_1, τ_1 are derived from the "Two-point Method" [42], which is described as follows.

Here, we denote y_0 as the initial temperature and $y(\infty)$ as the steady state value of the output temperature $y(t)$, and ΔU_0 the step input change. Then the process gain is obtained as $K_1 = (y(\infty) - y_0)/\Delta U_0$.

For the first order plus dead time in (1), we can derive the output $y(t)$ in the time domain as

$$y(t) = \begin{cases} 0, & t < \tau_1 \\ K_1 - K_1 e^{-\frac{t-\tau_1}{T_1}}, & t \geq \tau_1 \end{cases} \tag{3}$$

By choosing two points of $y(t_1) = 0.39(y(\infty) - y_0) + y_0$, $y(t_2) = 0.63(y(\infty) - y_0) + y_0$ and here $\tau_1 < t_1 < t_2$, T_1, τ_1 can be calculated as

$$\begin{aligned} T_1 &= 2(t_2 - t_1) \\ \tau_1 &= 2t_1 - t_2 \end{aligned} \tag{4}$$

For the fractional order model in (2), the same value of the time delay is selected as $\tau_1 = \tau_2$, and the other parameters will be adjusted by choosing the less variance of the error between the step-response output of the process model and practical output temperature.

III. FRACTIONAL ORDER CONTROLLER DESIGN

A. FRACTIONAL ORDER MODEL

Consider the aforementioned model shown in (2), the Oustaloup approximation [35], [40], [41] is applied to deal with the fractional order model. The Oustaloup approximation is given as

$$s^{\alpha} \approx K' \prod_{k=1}^{N} \frac{s + w'_k}{s + w_k} \quad (0 < \alpha < 1) \tag{5}$$

where,

$$\begin{aligned} K' &= w_h^{\alpha}, \quad w'_k = w_b w_u^{(2k-1-\alpha)/N}, \\ w_k &= w_b w_u^{(2k-1+\alpha)/N}, \quad w_u = \sqrt{w_h / w_b} \end{aligned}$$

and N is the approximation limit that relies on the orders of high order integer transfer function approximated by the fractional order derivative operator, w_b, w_h are the lower and higher frequency approximation interval. In the approximation method, the computation will be heavier by increasing the value of N, and in return, the approximation ripple may be eliminated.

The zero-order holder is added to discretize the derived high order model with the sampling time T_S, then the discrete form is

$$\begin{aligned} &y(k) + F_1 y(k-1) + F_2 y(k-2) + \cdots + F_n y(k-n) \\ &\quad = H_0 u(k-d) + H_1 u(k-d-1) + H_2 u(k-d-2) \\ &\qquad + \cdots + H_m u(k-d-m) \end{aligned} \tag{6}$$

where, $d = \tau / T_S$, $F_i (i = 1, 2, \cdots, n)$, $H_j (j = 0, 1, \cdots, m)$ are the coefficients of the discrete model, $y(k)$ is the output variable of the current instant, $y(k-1)$, $y(k-2)$, $\cdots$, $y(k-n)$ and $u(k-d)$, $u(k-d-1)$, $\cdots$, $u(k-d-m)$ are the outputs and inputs at the past corresponding time instants respectively.

The difference operator $\Delta = 1 - z^{-1}$ is added to (6), then we obtain

$$\begin{aligned} &\Delta y(k) + F_1 \Delta y(k-1) + F_2 \Delta y(k-2) + \cdots + F_n \Delta y(k-n) \\ &= H_0 \Delta u(k-d) + H_1 \Delta u(k-d-1) + H_2 \Delta u(k-d-2) \\ &\quad + \cdots + H_m \Delta u(k-d-m) \end{aligned} \tag{7}$$

A state space is chosen as

$$\begin{aligned} \Delta x(k) = [&\Delta y(k), \Delta y(k-1), \cdots, \Delta y(k-n), \\ &\Delta u(k-1), \cdots, \Delta u(k-d-m+1)]^{\mathrm{T}} \end{aligned} \tag{8}$$

Then the state space model is derived

$$\begin{aligned} \Delta x(k+1) &= A \Delta x(k) + B u(k) - B u(k-1) \\ \Delta y(k+1) &= C \Delta x(k+1) \end{aligned} \tag{9}$$

where,

$$A = \begin{bmatrix} -F_1 & \cdots & -F_{n-1} & -F_n & 0 & \cdots & 0 & H_0 & \cdots & H_{m-1} & H_m \\ 1 & 0 & \cdots & \cdots & 0 & \cdots & & 0 & \cdots & & 0 \\ 0 & \ddots & \ddots & & \vdots & & & \cdots & & \cdots & \vdots \\ \vdots & \ddots & 1 & 0 & \vdots & \cdots & & \cdots & & \cdots & \vdots \\ 0 & \ddots & 0 & 0 & 0 & & \cdots & & \cdots & & 0 \\ 0 & & \ddots & 0 & 1 & 0 & \cdots & & \cdots & & 0 \\ \vdots & \ddots & \ddots & & 0 & 1 & 0 & & & & \vdots \\ & \ddots & \ddots & \ddots & \ddots & & \ddots & \ddots & & \ddots & \\ \vdots & & \ddots & & & & \ddots & \ddots & & & \vdots \\ & \ddots & \ddots & \ddots & \ddots & \ddots & \ddots & & \ddots & \ddots & \\ 0 & & \cdots & & \cdots & 0 & \cdots & \cdots & 0 & 1 & 0 \end{bmatrix}$$

$$B = \begin{bmatrix} 0 & \cdots & 0 & 1 & 0 & \cdots & 0 \end{bmatrix}^{\mathrm{T}},$$

$$C = \begin{bmatrix} 1 & 0 & 0 & \cdots & \cdots & 0 \end{bmatrix}$$

B. FPFC CONTROLLER DESIGN

We denote

$$e(k) = y(k) - r(k) \tag{10}$$

where, $r(k)$ is the desired output at k time instant, $y(k)$ is the process output, $e(k)$ is the error between the process output and the desired output.

Remark 1: It is seen in (9) that unlike the method shown in [35] that adopts an Controlled Auto Regressive Integrated Moving Average (CARIMA) model, a systematic state space model is derived for further controller design, which will facilitate the controller design to use the state information.

The manipulated variable is performed through linear combination of the chosen basis functions. The form of the manipulated variable can be formulated as follows.

$$u(k+i) = \sum_{j=1}^{M} \mu_j f_j(i) \tag{11}$$

where, μ_j is the weight coefficient, $f_j(i)$ is the value of the basis function at the time instant $k+i$, M is the number of the basis function.

Combine (9), (10) and (11), the future error at time instant $k+i(i=1,2,\cdots,P)$ can be derived

$$\begin{aligned}
e(k+1) &= e(k) + \Delta y(k+1) - \Delta r(k+1) \\
&= e(k) + CA\Delta x(k) + CB\sum_{j=1}^{M}\mu_j f_j(0) - CBu(k-1) \\
&\quad - \Delta r(k+1) \\
e(k+2) &= e(k+1) + \Delta e(k+2) \\
&= e(k) + CA\Delta x(k) + CB\sum_{j=1}^{M}\mu_j f_j(0) - CBu(k-1) \\
&\quad -\Delta r(k+1) + \Delta y(k+2) - \Delta r(k+2) \\
&= e(k) + (CA^2+CA)\Delta x(k) + CAB\sum_{j=1}^{M}\mu_j f_j(0) \\
&\quad + CB\sum_{j=1}^{M}\mu_j f_j(1) - (CAB+CB)u(k-1)) \\
&\quad - \Delta r(k+1) - \Delta r(k+2) \\
&\vdots \\
e(k+P) &= e(k+P-1) + \Delta e(k+P) \\
&= e(k) + (CA^P + CA^{P-1} + \cdots + CA)\Delta x(k) \\
&\quad + [CA^{P-1}B\sum_{j=1}^{M}\mu_j f_j(0) + CA^{P-2}B\sum_{j=1}^{M}\mu_j f_j(1) \\
&\quad + \cdots + CB\sum_{j=1}^{M}\mu_j f_j(P-1)] \\
&\quad - (CA^{P-1}B + CA^{P-2}B + \cdots + CB)u(k-1) \\
&\quad - \Delta r(k+1) - \Delta r(k+2) - \cdots - \Delta r(k+P)
\end{aligned} \tag{12}$$

where, P is prediction horizon.

For the general PFC algorithm, the optimal cost function will be degraded as

$$\begin{aligned}
J &= \min \sum_{i=P_1}^{P_2} [r(k+i) - y(k+i)]^2 \\
&= \min \sum_{i=P_1}^{P_2} [e(k+i)]^2
\end{aligned} \tag{13}$$

$$r(k+i) = \beta^i y(k) + (1-\beta^i)c(k) \tag{14}$$

where, $[P_1, P_2]$ contains the coincidence points to be optimized, $c(k)$ is the set-point, $y(k+i)$ is the predicted output at time instant $k+i$, β is the smoothing factor of the reference trajectory, and $r(k+i)$ is the reference trajectory at the corresponding time instant.

For the fractional order calculus, it can be introduced into the fractional order cost function to replace (13) as

$$\begin{aligned}
J &= {}^{\gamma}I_{P_1T_S}^{P_2T_S}[e(t)]^2 \\
&= \int_{P_1T_S}^{P_2T_S} {}^{\gamma-1}I_{P_1T_S}^{P_2T_S}[e(t)]^2 dt \\
&= \int_{P_1T_S}^{P_2T_S} D^{1-\gamma}[e(t)]^2 dt
\end{aligned} \tag{15}$$

where, γ is the order of the fractional integral and $e(t)$ is the continuous error between the output and reference trajectory in the time domain. For simplicity, we denote ${}^{\gamma}I \equiv D^{-\gamma}$, where ${}^{\gamma}I$ is the fractional order integral notation and $D^{-\gamma}$ is the negative derivative notation.

Then the fractional order integral operator can be discretized using GL definition (seen in [27] and [33]):

$$\begin{aligned}
J \approx\ & T_S^{\gamma}[\omega_0^{(-\gamma)}e(k+P_2)^2 + \omega_1^{(-\gamma)}e(k+P_2-1)^2 \\
& + \cdots + (\omega_{P_2-P_1}^{(-\gamma)} - \omega_0^{(-\gamma)})e(k+P_1)^2 \\
& + (\omega_{P_2-P_1+1}^{(-\gamma)} - \omega_1^{(-\gamma)})e(k+P_1-1)^2 \\
& + \cdots + (\omega_{P_2-1}^{(-\gamma)} - \omega_{P_1-1}^{(-\gamma)})e(k+1)^2 \\
& + (\omega_{P_2}^{(-\gamma)} - \omega_{P_1}^{(-\gamma)})e(k)^2 + \cdots]
\end{aligned} \tag{16}$$

At current time instant k, $e(k)$ and the past error $e(k-1)$, etc., are all known values, then the cost function in the prediction interval $[P_1, P_2]$ can be simplified as follows

$$\begin{aligned}
J \approx\ & T_S^{\gamma}[\omega_0^{(-\gamma)}e(k+P_2)^2 + \omega_1^{(-\gamma)}e(k+P_2-1)^2 \\
& + \cdots + \omega_{P_2-P_1-1}^{(-\gamma)}e(k+P_1+1) \\
& + (\omega_{P_2-P_1}^{(-\gamma)} - \omega_0^{(-\gamma)})e(k+P_1)^2] \\
=\ & E^T W E
\end{aligned} \tag{17}$$

where,

$$\begin{aligned}
E &= [e(k+P_1), e(k+P_1+1), \cdots, e(k+P_2)]^{\mathrm{T}} \\
W &= T_S^{\gamma}\, diag(\omega_{P_2-P_1}^{(-\gamma)} - \omega_0^{(-\gamma)}, \\
&\quad \omega_{P_2-P_1-1}^{(-\gamma)}, \cdots, \omega_1^{(-\gamma)}, \omega_0^{(-\gamma)})
\end{aligned}$$

$$\omega_0^{(-\gamma)} = 1, \quad \omega_j^{(-\gamma)} = (1 - \frac{1-\gamma}{j})\omega_{j-1}^{(-\gamma)} \quad \text{for } \forall j > 0, \text{ and}$$

$$\omega_j^{(-\gamma)} = 0 \quad \text{for } j < 0.$$

Remark 2: It shows that the general fractional cost function is adopted in (15), which is different from the integer form of the cost function in [35] and more tuning of degrees can be offered compared with [35].

By minimizing the cost function in (17), the optimal control vector can be obtained as

$$\begin{aligned}
U = -(\psi^{\mathrm{T}}W\psi)^{-1}\psi^{\mathrm{T}}W[&L(y(k) - r(k)) + G\Delta x(k) \\
&- Su(k-1) - Q\Delta R]
\end{aligned} \tag{18}$$

$$S = \begin{bmatrix} CA^{P_1-1}B + CA^{P_1-2}B + \cdots + CB \\ CA^{P_1}B + CA^{P_1-1}B + \cdots + CB \\ \vdots \\ CA^{P_2-1}B + CA^{P_2-2}B + \cdots + CB \end{bmatrix} \tag{19a}$$

$$G = \begin{bmatrix} CA^{P_1} + CA^{P_1-1} + \cdots + CA \\ CA^{P_1+1} + CA^{P_1} + \cdots + CA \\ \vdots \\ CA^{P_2} + CA^{P_2-1} + \cdots + CA \end{bmatrix} \tag{19b}$$

$$L = [1 \quad 1 \quad \cdots \quad 1]^{\mathrm{T}} \tag{19c}$$

$$\psi = \begin{bmatrix} CBf_1(P_1-1) + \sum_{l=1}^{P_1-1} CA^j Bf_1(P_1-1-l) & CBf_2(P_2-1) + \sum_{l=1}^{P_1-1} CA^j Bf_2(P_1-1-l) & \cdots & CBf_M(P_1-1) + \sum_{l=1}^{P_1-1} CA^j Bf_M(P_1-1-l) \\ CBf_1(P_1) + \sum_{l=1}^{P_1} CA^j Bf_1(P_1-l) & CBf_2(P_1) + \sum_{l=1}^{P_1} CA^j Bf_2(P_1-l) & \cdots & CBf_M(P_1) + \sum_{l=1}^{P_1} CA^j Bf_M(P_1-l) \\ \vdots & \vdots & \cdots & \vdots \\ CBf_1(P_2-1) + \sum_{l=1}^{P_2-1} CA^j Bf_1(P_2-1-l) & CBf_2(P_2-1) + \sum_{l=1}^{P_2-1} CA^j Bf_2(P_2-1-l) & \cdots & CBf_M(P_2-1) + \sum_{l=1}^{P_2-1} CA^j Bf_M(P_2-1-l) \end{bmatrix} \tag{19d}$$

$$Q = \begin{bmatrix} 1 & 1 & \cdots & 1 & 0 & \cdots & 0 \\ 1 & 1 & \ddots & \ddots & \ddots & \ddots & \vdots \\ \vdots & \vdots & \ddots & \ddots & \ddots & \ddots & 0 \\ 1 & 1 & \cdots & 1 & \cdots & \cdots & 1 \end{bmatrix} \tag{19e}$$

$$U = [\mu_1, \mu_2, \cdots, \mu_M]^{\mathrm{T}} \tag{19f}$$

$$\Delta R = [\Delta r(k+1) \quad \Delta r(k+2) \quad \cdots \quad \Delta r(k+P)]^{\mathrm{T}} \tag{19g}$$

where (19a)–(19g), as shown at the top this page, where, Q is the matrix of $(P_2 - P_1 + 1) \times P_2$ dimension.

If we denote

$$\begin{aligned} \mu_1 &= -(1, 0, \cdots, 0)(\psi^T W \psi)^{-1} \psi^T W [L(y(k) \\ &\quad - r(k)) + G\Delta x(k) - Su(k-1) - Q\Delta R] \\ &= -h_1[y(k) - r(k)] - g_1 \Delta x(k) + v_1 u(k-1) - q_1 \Delta R \\ \mu_2 &= -(0, 1, \cdots, 0)(\psi^T W \psi)^{-1} \psi^T W [L(y(k) \\ &\quad - r(k)) + G\Delta x(k) - Su(k-1) - Q\Delta R] \\ &= -h_2[y(k) - r(k)] - g_2 \Delta x(k) + v_2 u(k-1) - q_2 \Delta R \\ &\vdots \\ \mu_M &= -(0, 0, \cdots, 1)(\psi^T W \psi)^{-1} \psi^T W [L(y(k) \\ &\quad - r(k)) + G\Delta x(k) - Su(k-1) - Q\Delta R] \\ &= -h_M[y(k) - r(k)] - g_M \Delta x(k) + v_M u(k-1) \\ &\quad - q_M \Delta R \end{aligned} \tag{20}$$

Then the manipulated variable at the current time instant can be derived as

$$u(k) = -H_y[y(k) - r(k)] - G_x \Delta x(k) + V_u u(k-1) - Q_u \Delta R \tag{21}$$

where,

$$\begin{aligned} H_y &= \sum_{j=1}^{M} h_j f_j(0) \\ G_x &= \sum_{j=1}^{M} g_j f_j(0) \\ V_u &= \sum_{j=1}^{M} v_j f_j(0) \\ Q_u &= \sum_{j=1}^{M} q_j f_j(0) \end{aligned} \tag{22}$$

Remark 3: It is noted that the merits of both the fractional order PID algorithm and predictive control algorithms can be integrated for improved control performance, which is a smart way of combining both the PID performance and the prediction function. The future work of the proposed method can borrow such ideas and such that the resultant controller will both bear the performance of the proposed fractional order PFC and the PID controller.

IV. APPLICATION ON INDUSTRIAL HEATING FURNACE

In this section, the performance of the proposed fractional order controller will be verified on the practical electric heating furnace.

A. PROCESS DESCRIPTION

The overall diagram of the experimental device for the temperature process control system is shown in Fig.1. It mainly consists of an electric heating furnace SXF-4-10, an industrial personal computer (IPC) 610L, and several connected devices, such as the signal amplifier, the solid state relay, the terminal strip, etc. The active functions of these components will be formulated in the following details. The flow chart of the temperature control system is displayed in Fig.2, where the brief description is as follows.

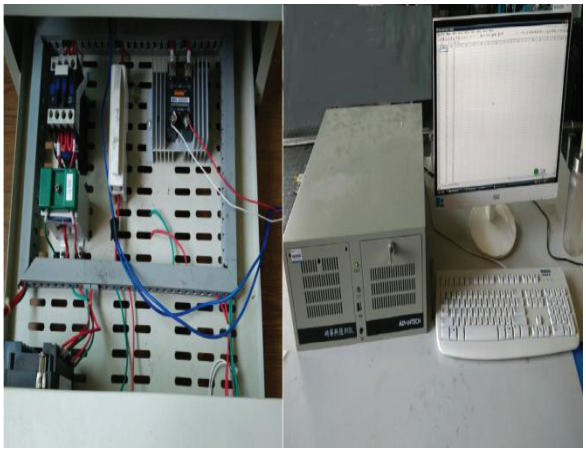

FIGURE 1. The diagram of wiring connection and industrial personal computer 610L.

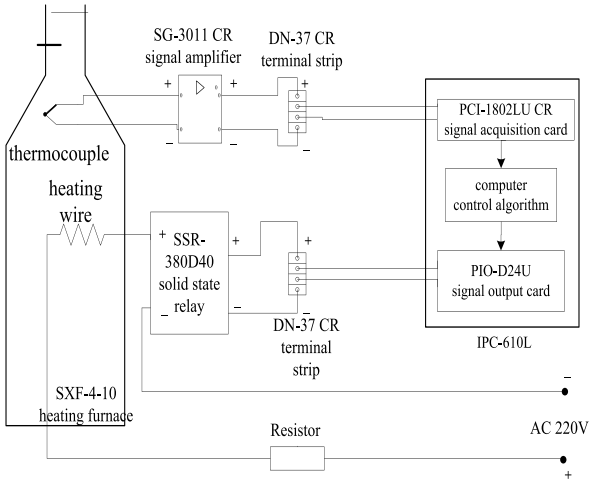

FIGURE 2. Process flow chart of the electric heating furnace (SXF-4-10).

The overall temperature process mainly consists of the measurement module and the heating module. The two modules have been connected by a computer that contains the process control algorithm and the transformation rule between real-time temperature and the corresponding voltage. In the measurement module, the thermocouple is used to implement the temperature measurement function while the PCI-1802LU CR signal acquisition card is employed to collect the voltage corresponding to the real-time temperature data. Since the voltage is too small to be recognized, the SG-3011CR signal amplifier has been added to amplify the voltage signal to avoid tremendous measurement error. In the heating module, the temperature is controlled by on-off control of the SSR-380D40 solid state relay. The PIO-D24U signal output card is used to transmit the corresponding voltage signal to the solid-state relay. When the input digital signal of the PIO-D24U card is set to 0x01 by the computer, the +5V output voltage will be obtained by solid state relay. Then the SSR-380D40 relay is on-state and the SFX 4-10 electric heating furnace is on heating state. On the contrary, if the input digital signal is 0x00, the output voltage of signal output card is 0V and the SSR-380D40 is at off-state. Then the circuit of the heating module is switch-off and the heating wire of furnace does not work. In addition, the DN-37 CR terminal strip is used to transmit the voltage and the resistor is added to divide the AC voltage.

B. MANIPULATED VARIABLE

In the IPC, the error between the practical measurement temperature and the temperature set-point is seen as the input of the control algorithm and the output of the computer is the percentage, namely duty ratio (dr) of the heating state for the heating furnace during the selected heating time nT_S, where $T_S = 10s$ is the sampling time and n is the number of heating time. Within the current heating cycles nT_S, the duty ratio dr will be performed on the output temperature. In other words, SSR-380D40 relay is on-state if the input digital signal is 0x01 during the time $dr \cdot nT_S$, while the relay is at off-state when the input signal is 0x00 during the remaining time $(1 - dr) \cdot nT_S$.

The duty ratio dr calculated by comparing the set-point with the practical measurement temperature is seen as the manipulated variable for the temperature control process and the time for heating or the on-state of the solid-state relay depends on the duty ratio of the heating cycles. In the next nT_S heating cycles, the loop will start again.

C. CONTROL PROBLEM

From the perspective of practical consideration, the PID method is applied to stabilize the temperature of the heating furnace. In view of the overall process, the output of PID is regarded as the manipulated variable, i.e., the duty ratio, which will be transformed into the corresponding voltage by IPC. Then the value of the voltage will be used to determine the on-off state of the solid-state relay. Thus, the appropriate heating time when the solid-state relay is on-state will be obtained for heating furnace.

The proposed FPFC algorithm is based on the generalized process involving the PID close-loop feedback system. The structure of the proposed method is shown in Fig.3,

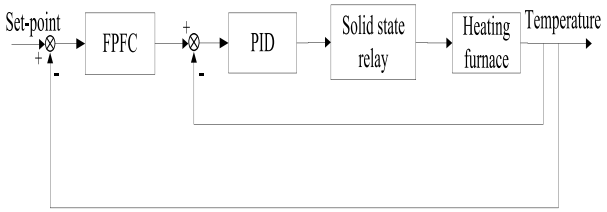

FIGURE 3. Control block of FPFC-PID for heating furnace.

where the input of PID will be the output of the fractional order controller and the input of the FPFC is seen as the difference between the process output temperature and the temperature set-point.

For the realization of this control process, the programmed control algorithm is the main bridge that connects the input-output data to the whole process. The automated implementation for the temperature control system is shown in Fig. 4. In this application, the proposed FPFC method is realized over the original internal-model PID in the computer program, where the real-time temperature is transmitted to the function of the proposed FPFC and PID function is communicated by calling the function module of FPFC. Then the program of FPFC-PID module is successful connected. For simplicity, the process model is obtained off-line, where the control parameters of S, G, L, F_i, H_j, Q, W can be derived before the real-time experiments based on the aforementioned parameters, such as β, P, etc. In Fig.4, the whole control program consists of the conversion program between the duty ratio and the heating time, the off-line calculated program, the real-time temperature access program and the main output control program of the control variable. The data access program is to acquire the real-time temperature from the heating furnace using the thermocouple and transmit the corresponding temperature to the control program, while the control program will calculate the duty ratio by combining the offline calculation and real-time temperature. Then the duty

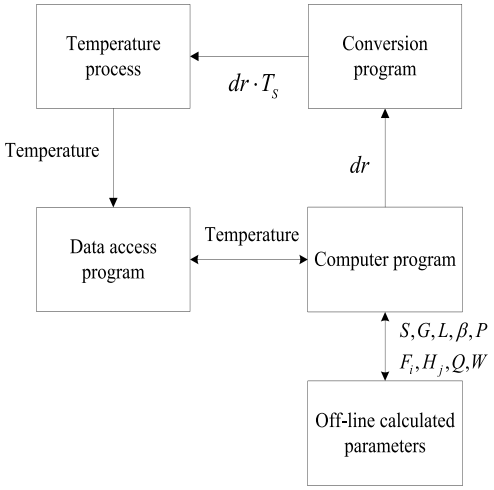

FIGURE 4. Automated implementation for the temperature control system.

ratio will be transformed into the corresponding voltage and the heating time $dr \cdot nT_S$ determined by the voltage will be performed on the electric heating furnace.

D. PROCESS MODEL

The two process models, that is, integer first order model and fractional order model, can be modeled through the practical input-output temperature of the electric heating furnace, where the input data is the set-point of the internal-model PID, and the output data is the practical measured temperature. As can be seen in [39], internal model control (IMC) was introduced into the design of PID control and the tuning parameters of PID control are chosen as

$$K_p = \frac{(T + 0.5\tau)}{K(\lambda + 0.5\tau)}, \quad T_i = T + 0.5\tau, \; T_d = \frac{T\tau}{2T + \tau} \tag{23}$$

where, K, T, τ are the parameters of the heating furnace. λ is an extra parameter with $\lambda > 0.8\tau$. To satisfy the requirement of the performance of the heating furnace, i.e., the settling time, overshoots and fluctuation of the response, the parameters of the PID for the heating furnace are derived as $K_p = 2.74, K_i = 0.0036, K_d = 0$. The response is done with the set-point of PID changing from indoor temperature to 300° for process modeling.

The integer first order plus dead time model based on the step response of the process output is

$$G_1(s) = \frac{1}{600s + 1} e^{-100s} \tag{24}$$

The corresponding fractional order model is

$$G_2(s) = \frac{1}{500s^{0.95} + 1} e^{-100s} \tag{25}$$

According to the Oustaloup approximated method in Eq.(5) and the experimental chosen parameters as $N = 4$, $w_b = 10^{-6}$, $w_h = 10^6$, the Oustaloup approximation model can be derived with

$$G_3(s) = \frac{s^4 + a_1 s^3 + a_2 s^2 + a_3 s + a_4}{b_1 s^4 + b_2 s^3 + b_3 s^2 + b_4 s + b_5} e^{-100s} \tag{26}$$

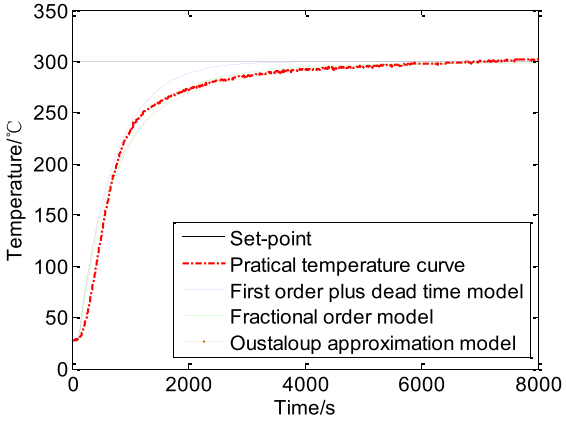

FIGURE 5. Step responses of the models and practical temperature of the furnace.

where,

$$a_1 = 8.422 \times 10^5, \quad a_2 = 7.087 \times 10^8,$$
$$a_3 = 5.963 \times 10^8, \quad a_4 = 5.012 \times 10^5$$
$$b_1 = 2.506 \times 10^8, \quad b_2 = 2.981 \times 10^{11},$$
$$b_3 = 3.55 \times 10^{11}, \quad b_4 = 1.017 \times 10^9, \; b_5 = 5.017 \times 10^5$$

The responses of the three models and the real-time temperature output response are shown in Fig. 5. The statistical results of the step-response models are listed in Table 1. It is found that the fractional order model and its approximated Oustaloup model are more precise to match the practical output temperature than the integer first order model.

TABLE 1. Statistical Measures of the Step-Response Models

type	standard variance	root mean squared error	median
Fractional order model	6.3720	6.3721	2.0169
Oustaloup approximation model	7.2625	7.3031	2.8224
First order plus dead time mode	8.1868	10.382	5.0855

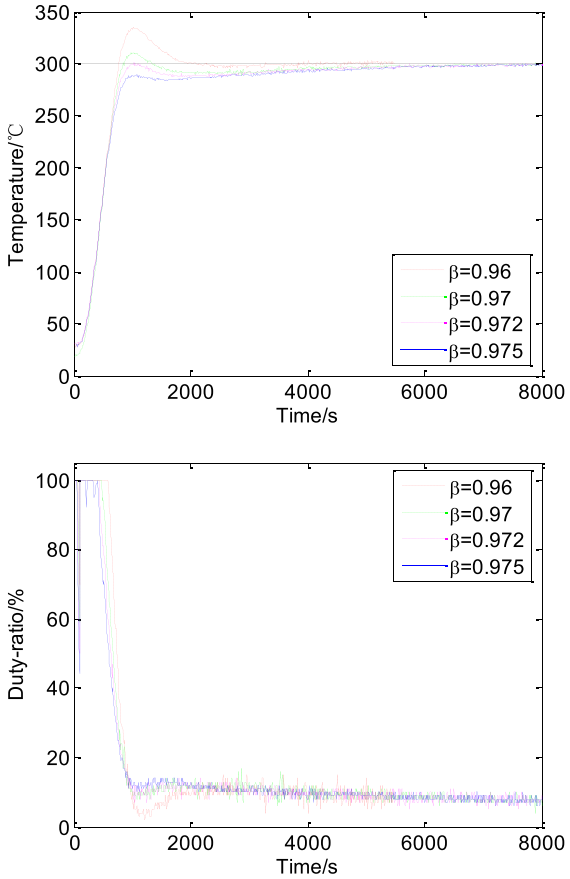

FIGURE 6. Close-loop responses of the proposed FPFC for variation in β.

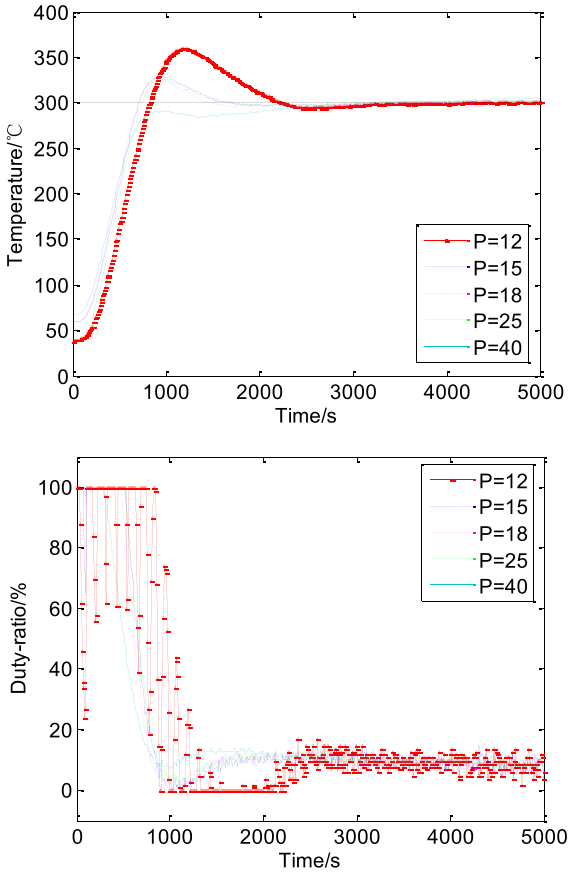

FIGURE 7. Closed-loop responses of the proposed FPFC for variation in P.

Here we use the absolute value of difference $\Delta SE_i = |y_p(i) - y_m(i)|$ between the practical measured data and the step-response model output at each sampling time to evaluate the models in Table 1, where $y_p(i)$, $y_m(i)$ are the practical measured temperature and the step-response model output at sampling time instant i, $(i = 1, 2, \cdots, L_s)$, respectively. The results of standard variance of the step-response models have been carried out via (27a) and the root mean squared error is carried out via (27b), where $L_s = TF/T_s$ is the total sampling numbers with $TF = 8000$, and $\Delta\bar{S}\bar{E}$ is the average value of ΔSE_i.

$$SD = \sqrt{\sum_{i=1}^{L_s} (\Delta SE_i - \Delta\bar{S}\bar{E})^2/n} \tag{27a}$$

$$RMSE = \sqrt{\sum_{i=1}^{L_s} [y_p(i) - y_m(i)]^2/n} \tag{27b}$$

E. EXPERIMENTAL RESULTS

The PFC and proposed FPFC have been applied to the temperature of the electric heating furnace, where (24) and (26) are discretized for PFC and FPFC respectively and the sampling time is still selected as $T_S = 10s$. Then the two discrete

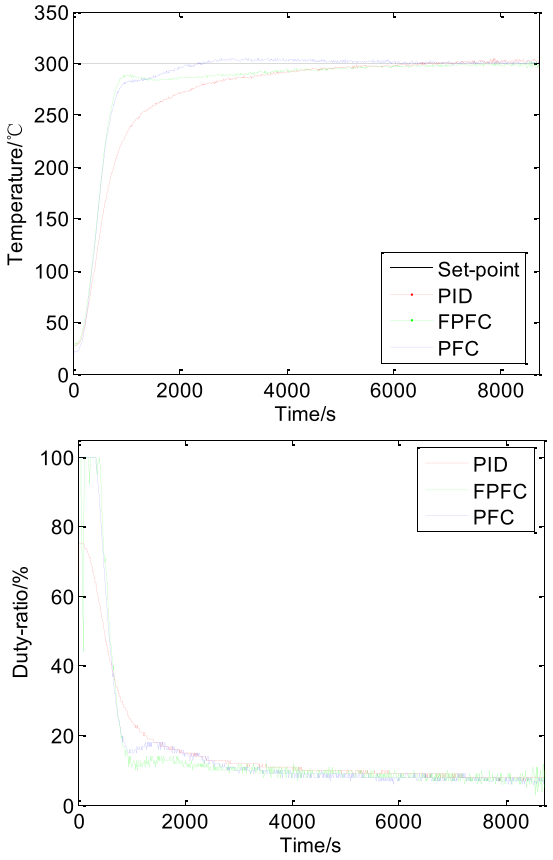

FIGURE 8. Performance of the set-point tracking of practical temperature control systems.

models can be derived respectively as follows

$$G_1(z) = \frac{0.01653}{z - 0.9835} z^{-10} \tag{28}$$

$$G_3(z) = \frac{a_{z0}z^4 + a_{z1}z^3 + a_{z2}z^2 + a_{z3}z + a_{z4}}{z^4 + b_{z1}z^3 + b_{z2}z^2 + b_{z3}z + b_{z4}} z^{-10}$$
$$a_{z0} = 3.991 \times 10^{-9}, \quad a_{z1} = 0.01722, \quad a_{z2} = -0.01765,$$
$$a_{z3} = 0.0005697, \quad a_{z4} = 5.482 \times 10^{-12},$$
$$b_{z1} = -1.972, \quad b_{z2} = 0.9717,$$
$$b_{z3} = -6.651 \times 10^{-6}, \quad b_{z4} = -6.333 \times 10^{-24} \tag{29}$$

To verified the merit of the proposed FPFC method, the more accurate approximated model in (29) which is derived from the fractional model is used for the design of the proposed controller. Using the fractional order cost function, the controller can be more flexible with more degrees of freedom. The following experiments have been implemented on the heating furnace.

For the set-point tracking, if a constant set-point is to be achieved, a step function can be selected. Otherwise, higher-order basis functions may be required if a ramp, parabolic, etc., set-point is required. Since the temperature is to track a constant profile, one step base function is selected. It means that $u(k+i) = \mu_1$. In the following experiments, the set-point is 300° from the time instant $k = 0$, and the prediction horizon is chosen as $P_1 = P_2 = P$.

In fact, the parameter γ is an arbitrary order. For simplicity, the fractional integral order is set as $\gamma = 0$ Then the design of FPFC will follow the general design strategy of PFC, i.e., multi-step prediction, feedback correction and receding horizon optimization.

Fig.6 depicts the performance of the control system for the variation in β when the prediction horizon is fixed as $P = 15$, and the experiment results shown in Fig.7 are for variation in P when β is fixed as $\beta = 0.95$. It is shown in Fig. 6 that the overshoots of the controller can be decreased by increasing β. In Fig.7, by increasing the parameter P from 12 to 40, the overshoots of closed-loop response for the proposed control system will be weakened. Even though the initial temperature of the heating furnace may be different in Figs.6 and 7, it can be negligible due to the fact that the initial values have no effect on the dynamic trends of the control response. Considering the overall effect of the two parameters, the relatively satisfactory values are chosen as $\beta = 0.975, P = 15$ to evaluate the performance of the proposed FPFC. The comparisons of the experiment results with the proposed fractional order controller and the other controllers are shown in Figs.8-10.

The performance of the set-point tracking of the control systems from indoor temperature to the preset temperature is

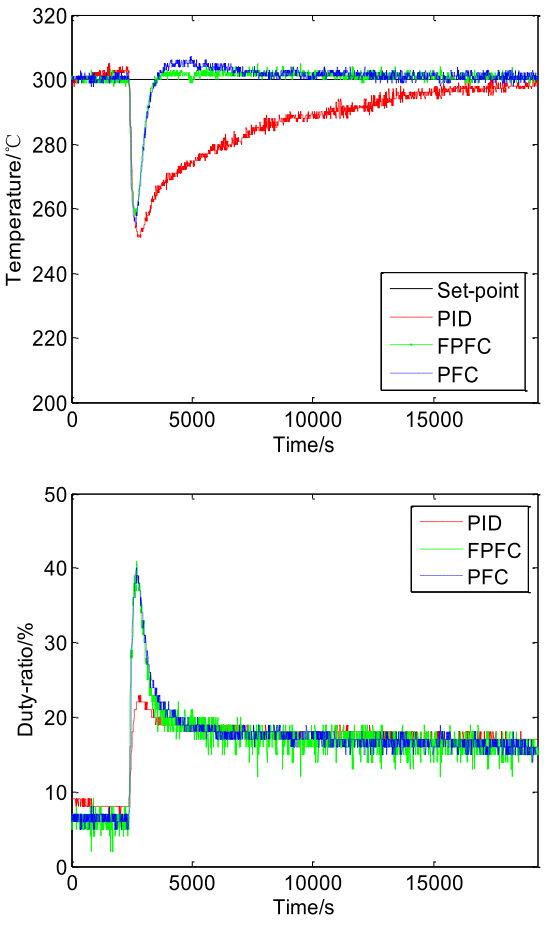

FIGURE 9. Performance of the disturbance rejection of practical temperature control systems.

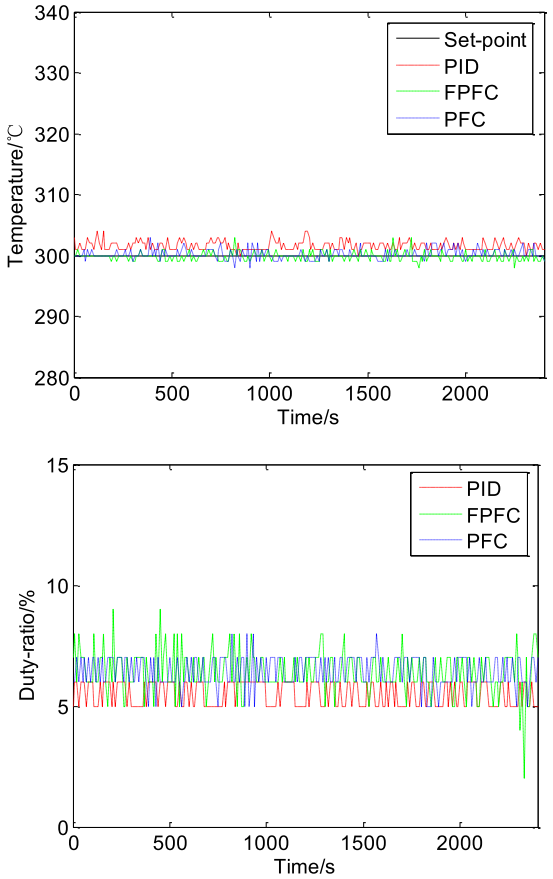

FIGURE 10. Experimental tests of steady state performance for practical temperature control systems.

shown in Fig.8, which shows the output temperature of the close-loop systems and the corresponding input duty ratio. The faster responses are obtained for both the PFC and the proposed FPFC as compared with classical PID. It is seen that the proposed FPFC yields no overshoot and act better than the integer PFC with overshoots of the maximum value of $(307 - 300)/300$.

To verify the performance of the disturbance rejection, a small mouth of the door of the electric heating furnace is opened to connect with the outer space. Fig.9 shows that the proposed FPFC gives the best disturbance rejection although these methods can reject this disturbance and force the temperature to track the required set-point again. The PID close-loop control system recovers to the set-point at the expense of the longest time of nearly five hours. Faster recoverability of disturbance rejection is obtained for both PFC and the proposed FPFC. Even more, the PFC shows greater overshoots as compared with the proposed FPFC.

In Fig.10, the experimental tests regarding the steady state performance of the practical control systems are discussed. It can be seen that the residual error will exist by PID controller, and the temperature of the proposed fractional order control system will be preferably maintained within the desired output. In addition, Table 2 shows more clearly the corresponding computed results regarding average, maximum, minimum, standard deviation and extreme deviation of the output temperature. The experimental results show improved performance of the proposed FPFC strategy. Moreover, the computation time of the control action calculation of the three methods are also calculated, and they are 0.684s, 0.53s and 0.42s for FPFC, PFC and PID respectively. It shows that it is acceptable for real-time application although the computational burden of FPFC is the heaviest.

TABLE 2. Statistical Results of Output Temperature

Statistical Measures	PID	FPFC	PFC
Average	301.62	299.78	300.26
Maximum	304	303	303
Minimun	300	298	298
Stardard Deviation	0.78534	0.66739	0.80468
Extreme Deviation	0.84563	0.80593	0.8948
Median	301	300	300
Root Mean Squared Error	1.8025	0.70269	0.8448

V. CONCLUSION

In this paper, an approach of fractional order PFC is proposed and the application has been implemented on an electric heating furnace. The proposed method is based on the fractional order model and the state space model is used to derive the predictive functional control law. The experimental results on the temperature process reveal the improvement of the proposed FPFC method. As there is no quantitative analysis for tuning parameters of predictive control, the tuning parameters of the controller were chosen depending on experience in practice. In a way, the more effective prediction model can be derived from the more precise fractional order model which is a baseline for FPFC controller. With the additional freedom degree, the performance of the controller can be improved by adjusting the suitable fractional-order value.

REFERENCES

[1] W. Trinks, M. H. Mawhinney, R. A. Shannon, R. J. Reed, and J. R. Garvey, *Industrial Furnaces*, 6th ed. Hoboken, NJ, USA: Wiley, 2004.
[2] Y. H. Duan, "The design of predictive fuzzy-PID controller in temperature control system of electrical heating furnace," in *Proc. Int. Conf. Intell. Comput. Sustain. Energy Environ.* Berlin, Germany: Springer, 2010, pp. 259–265.
[3] W. Tan, J. Liu, T. Chen, and H. J. Marquez, "Comparison of some well-known PID tuning formulas," *Comput. Chem. Eng.*, vol. 30, no. 9, pp. 1416–1423, Jul. 2006.
[4] K. G. Begum, A. S. Rao, and T. K. Radhakrishnan, "Enhanced IMC based PID controller design for non-minimum phase (NMP) integrating processes with time delays," *ISA Trans.*, vol. 68, pp. 223–234, Jul. 2017.
[5] X. Zhou, J. Zhou, C. Yang, and W. Gui, "Set-point tracking and multi-objective optimization-based PID control for the goethite process," *IEEE Access*, vol. 6, pp. 36683–36698, 2018.
[6] R. Zhang, R. Lu, A. Xue, and F. Gao, "New minmax linear quadratic fault-tolerant tracking control for batch processes," *IEEE Trans. Autom. Control*, vol. 61, no. 10, pp. 3045–3051, Oct. 2016.

[7] H.-G. Han, L. Zhang, and J.-F. Qiao, "Data-based predictive control for wastewater treatment process," *IEEE Access*, vol. 6, pp. 1498–1512, 2018.
[8] Y. A. Sha'aban, F. Tahir, P. W. Masding, J. Mack, and B. Lennox, "Control improvement using MPC: A case study of pH control for brine dechlorination," *IEEE Access*, vol. 6, pp. 13418–13428, 2018.
[9] R. D. Zhang, A. K. Xue, and F. R. Gao, "Temperature control of industrial coke furnace using novel state space model predictive control," *IEEE Trans. Ind. Informat.*, vol. 10, no. 4, pp. 2084–2092, Nov. 2014.
[10] R. Zhang, S. Wu, Z. Cao, J. Lu, and F. Gao, "A systematic min–max optimization design of constrained model predictive tracking control for industrial processes against uncertainty," *IEEE Trans. Control Syst. Technol.*, vol. 26, no. 6, pp. 2157–2164, Nov. 2018.
[11] V. Mahindrakar and J. Hahn, "Model predictive control of reactive distillation for benzene hydrogenation," *Control Eng. Pract.*, vol. 52, pp. 103–113, Jul. 2016.
[12] Q. Xu and S. Dubljevic, "Model predictive control of solar thermal system with borehole seasonal storage," *Comput. Chem. Eng.*, vol. 101, pp. 59–72, Jun. 2017.
[13] J. Richalet, S. A. El Ata-Doss, C. Arber, H. B. Kuntze, A. Jacubasch, and W. Schill, "Predictive functional control—Application to fast and accurate robots," *IFAC Proc. Vol.*, vol. 20, no. 5, pp. 251–258, Jul. 1987.
[14] J. Richalet and D. O'Donovan, *Predictive Functional Control: Principles and Industrial Applications*, Heidelberg, Germany: Springer, 2009.
[15] R. Zhang and Q. Jin, "Design and implementation of hybrid modeling and PFC for oxygen content regulation in a coke furnace," *IEEE Trans. Ind. Informat.*, vol. 14, no. 6, pp. 2335–2342, Jun. 2018.
[16] A. Vivas and P. Poignet, "Predictive functional control of a parallel robot," *Control Eng. Pract.*, vol. 13, no. 7, pp. 863–874, Jul. 2005.
[17] R. D. Zhang, S. Wu, and J. L. Tao, "A new design of predictive functional control strategy for batch processes in the two-dimensional framework," *IEEE Trans. Ind. Inform.*, to be published, doi: 10.1109/TII.2018.2874711.
[18] G. Karer, I. Škrjanc, and B. Zupančič, "Self-adaptive predictive functional control of the temperature in an exothermic batch reactor," *Chem. Eng. Process., Process Intensification*, vol. 47, no. 12, pp. 2379–2385, Nov. 2008.
[19] S. Wang, J. Fu, Y. Yang, and J. Shi, "An improved predictive functional control with minimum-order observer for speed control of permanent magnet synchronous motor," *J. Electr. Eng. Technol.*, vol. 12, no. 1, pp. 272–283, Jan. 2017.
[20] Y. Wang, Q. Jin, and R. Zhang, "Improved fuzzy PID controller design using predictive functional control structure," *ISA Trans.*, vol. 71, pp. 354–363, Nov. 2017.
[21] K. Zabet and R. Haber, "Robust tuning of PFC (predictive functional control) based on first- and aperiodic second-order plus time delay models," *J. Process Control*, vol. 54, pp. 25–37, Jun. 2017.
[22] Q. Zhang, Q. Wang, and G. Li, "Nonlinear modeling and predictive functional control of Hammerstein system with application to the turntable servo system," *Mech. Syst. Signal Process.*, vols. 72–73, pp. 383–394, May 2016.
[23] J. A. Rossiter, R. Haber, and K. Zabet, "Pole-placement PFC (predictive functional control) for systems with one oscillatory mode," in *Proc. Eur. Control Conf.*, Aalborg, Denmark, Jun./Jul. 2016, pp. 776–781.
[24] M. Ö. Efe, "Fractional order systems in industrial automation—A survey," *IEEE Trans. Ind. Inform.*, vol. 7, no. 4, pp. 582–591, Nov. 2011.
[25] J.-D. Gabano and T. Poinot, "Fractional modelling and identification of thermal systems," *Signal Process.*, vol. 91, no. 3, pp. 531–541, Mar. 2011.
[26] N. Aguila-Camacho, J. D. Le Roux, M. A. Duarte-Mermoud, and M. E. Orchard, "Control of a grinding mill circuit using fractional order controllers," *J. Process Control*, vol. 53, pp. 80–94, May 2017.
[27] D. Wang and R. Zhang, "Design of distributed PID-type dynamic matrix controller for fractional-order systems," *Int. J. Syst. Sci.* , vol. 49, no. 2, pp. 435–448, Jan. 2018.
[28] B. M. Vinagre, C. A. Monje, A. J. Calderón, and J. I. Suárez, "Fractional PID controllers for industry application. a brief introduction," *J. Vib. Control*, vol. 13, nos. 9–10, pp. 1419–1429, Sep. 2007.
[29] M. Beschi, F. Padula, and A. Visioli, "Fractional robust PID control of a solar furnace," *Control Eng. Pract.*, vol. 56, pp. 190–199, Nov. 2016.
[30] C. Ma and Y. Hori, "Fractional-order control: Theory and applications in motion control," *IEEE Ind. Electron. Mag.*, vol. 1, no. 4, pp. 6–16, Dec. 2007.
[31] N. Bigdeli, "The design of a non-minimal state space fractional-order predictive functional controller for fractional systems of arbitrary order," *J. Process Control*, vol. 29, pp. 45–56, May 2015.
[32] M. Abdolhosseini and N. Bigdeli, "Predictive functional control for fractional order system," *Int. J. Electron. Commun. Comput. Eng.*, vol. 5, no. 1, pp. 16–23, Jan. 2014.
[33] M. Romero, A. P. de Madrid, C. Mañoso, V. Milanés, and B. M. Vinagre, "Fractional-order generalized predictive control: Application for low-speed control of gasoline-propelled cars," *Math. Problems Eng.*, vol. 2013, Jan. 2013, Art. no. 895640.
[34] M. Romero, A. P. de Madrid, C. Mañoso, and B. M. Vinagre, "Fractional-order generalized predictive control: Formulation and some properties," in *Proc. 11th Int. Conf. Control, Automat. Robot. Vis.*, Singapore, Dec. 2010, pp. 1495–1500.
[35] A. Rhouma, B. Bouzouita, and F. Bouani, "Practical application of model predictive control to fractional thermal system," in *Proc. 2nd Int. Conf. Informat. Appl.*, Lodz, Poland, Sep. 2013, pp. 222–227.
[36] W. Guo, J. Ni, T. Li, and L. Deng, "Improved fractional-order PID predictive function excitation controller based on time domain," *Chin. J. Sci. Instrum.*, vol. 32, no. 11, pp. 2461–2467, Nov. 2011.
[37] W. Guo, J. H. Wen, and W. P. Zhou, "Improved fractional order PID dynamic matrix control algorithm based on time domain," *Chin. J. Sci. Instrum.*, vol. 31, no. 5, pp. 968–973, May 2010.
[38] P. Sopasakis and H. Sarimveis, "Stabilising model predictive control for discrete-time fractional-order systems," *Automatica*, vol. 75, pp. 24–31, Jan. 2017.
[39] C. Zou, L. Zhang, X. Hu, Z. Wang, T. Wik, and M. Pecht, "A review of fractional-order techniques applied to lithium-ion batteries, lead-acid batteries, and supercapacitors," *J. Power Sources*, vol. 390, pp. 286–296, Apr. 2018.
[40] C. Zou, X. Hu, S. Dey, L. Zhang, and X. L. Tang, "Nonlinear fractional-order estimator with guaranteed robustness and stability for lithium-ion batteries," *IEEE Trans. Ind. Electron.*, vol. 65, no. 7, pp. 5951–5961, Jul. 2018.
[41] C. Zou, X. Hu, Z. Wei, T. Wik, and B. Egardt, "Electrochemical estimation and control for lithium-ion battery health-aware fast charging," *IEEE Trans. Ind. Electron.*, vol. 65, no. 8, pp. 6635–6645, Aug. 2018.
[42] B. W. Bequette, *Process Control: Modeling, Design, and Simulation*. Upper Saddle River, NJ, USA: Prentice-Hall, 2003.

XIAOMIN HU is currently an Associate Professor with the School of Science, Hangzhou Dianzi University, Hangzhou. She has published over 20 papers on system modeling, and control system design and analysis. Her research interests include modeling, system analysis, and control system design.

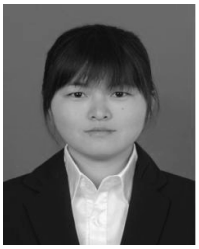

QIN ZOU is currently the Lecturer with the Automation Department, Hangzhou Dianzi University, Hangzhou. She has published over 10 papers on system identification and modeling, and control system design. Her research interests include system identification, process control, and control system design.

HONGBO ZOU is currently an Associate Professor with the Automation Department, Hangzhou Dianzi University, Hangzhou. He has published over 30 papers on robust control and model predictive control. His research interests include robust control, model predictive control, and control system design.